Earth's Cryosphere, 2016, vol. XX, No. 2, pp. 69–77 **http://earthcryosphere.ru/**

EFFICIENCY OF FINNING IN SHORT VERTICAL TWO-PHASE THERMOSYPHONS FOR CONSTRUCTION ON PERMAFROST

J.B. Gorelik, A.A. Seleznev

Earth Cryosphere Institute, SB RAS, P/O box 1230, Tyumen, 625000, Russia; gorelik@ikz.ru

A theoretical study is applied to related processes of heat and mass transfer inside and outside a cooling system for construction on permafrost: a vertical two-phase thermosyphon or Long's tube based on natural convection. The performance enhancement by finning on condenser units in such systems is limited by thermal resistance of condensate films that sink along the condenser inner wall. The efficiency of fins largely depends on the specific cooling agent and is the highest with ammonia. The maximum length of the evaporator tube corresponds to the point of zero condensate film thickness. The boundary condition on the evaporator outer wall makes basis for estimating the temperature dynamics of ground stabilized by thermosyphons. Unfinned thermosyphons turn out to be no less efficient than the finned systems, but have engineering and economic advantages due to avoiding additional costs and installation problems.

Thermosyphon, condenser, evaporator, two-phase flows, saturation temperature, thermal resistance, heat exchange, cooling

INTRODUCTION

Vertical two-phase systems of natural convection (thermosyphons) with a relatively short buried unit within 10–15 m are among most widely used cooling devices [*Vyalov, 1983; Makarov, 1985; Minkin, 2005; Dolgikh and Okunev, 2006*]. Such systems are based on the design of Long's thermo-valve piling [*Long, 1964*], which is quite simple (Fig. 1): a sealed hollow tubular vessel containing a pre-determined amount of a selected suitable liquid of low boiling point (cooling agent) is inserted into soil and has a long buried portion and a short (within 1.5–2.0 m) above-ground portion subjected to below freezing temperatures. The effect is to transfer heat away from the buried end portion [*Long, 1964*], by the following mechanism. During winter periods of subfreezing temperatures, the coolant in the buried portion of the system (evaporator) extracts heat from the adjoining permafrost and evaporates; the vapor rises to the colder above-ground portion of the system (condenser) dissipating heat to air, condenses on the tube surface, and returns to the lower end by gravity. The cycle repeats and leads to freezing of unfrozen soil and/or the lowering of the permafrost temperature, but it stops in summer. Special engineering solutions are applied to maintain year-round operation of such systems, or even to increase the cooling effect progressively: use of heat insulation and a sufficient number of tubes, etc., proceeding from special thermal design.

Such systems have been used in kilometers-long above-ground pipelines (the Trans-Alaska pipeline system or pipelines in northern West and East Siberia), and in numerous buildings and utility structures on permafrost in Russian Arctic oil and gas fields [*Dolgikh et al., 2004; Minkin, 2005*]. These systems are intended to cool down permafrost to a designed temperature and maintain this temperature (thermal stabilization) for the whole lifetime of the respective structures. They are most often installed prior to main construction, when foundations are being prepared. Thermosyphons are almost never used for the energy-consuming freezing of taliks, except for few cases of deeply buried systems for thermal stabilization of dam cores or for repairing thaw-related failures in the course of operation [*Dolgikh, 2014; Kutvitskaya and Minkin, 2014*]. Methods for thermal stabilization of discontinuous permafrost are of special interest [*Khrustalev and Ershov, 1999*].

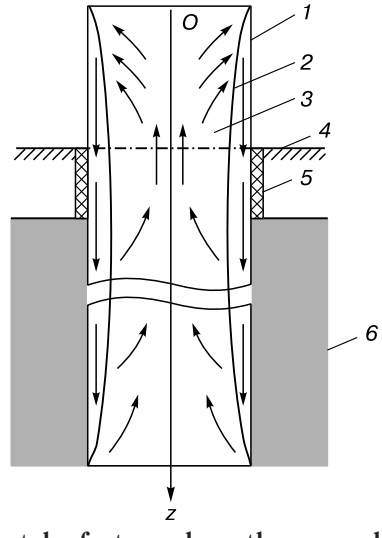

Fig. 1. Sketch of a two-phase thermosyphon.

1 – tubular case; *2*, *3* – cooling agent in liquid and vapor phases; *4* – active layer; *5* – heat insulation; *6* – frozen soil.

Copyright © 2016 J.B. Gorelik, A.A. Seleznev, All rights reserved.

The condenser unit can be equipped with heat absorption fins which are presumed to enhance the cooling effect, as it has been observed in practice. On the other hand, it follows from the theory (e.g., [*Arnold et al., 1979*]) that fins should be mounted on the side of the medium with worse thermal properties. Special research is needed to assess the potential efficiency of finning, given that heat transfer in thermosyphons is mainly by convection above the ground and by conduction in the buried end, from the ground which is known to have quite a low thermal conductivity. As far as we know, there is no data available to prove the thermal performance gain due specifically to fins. We expect to bridge the gap by this study.

HEAT EXCHANGE OF THERMOSYPHONS WITH GROUND AND WITH AIR

Heat transfer in thermosyphons should be modeled by considering jointly the processes inside (phase change and flow of coolant) and outside (heat exchange with ground and air) the cooling systems. The respective modeling suggested for the first time by *Gorelik* [*1980*] for an unfinned thermosyphon led to an ordinary third-kind boundary condition on the outer wall of the buried unit (evaporator). The boundary condition includes parameters of heat exchange with ground and air and makes basis for formulating and solving a broad scope of problems concerning ground temperature dynamics in permafrost foundations stabilized by single or multiple thermosyphons. The derivation for an unfinned system [*Gorelik, 1980*] is to be adapted to the case of finning.

CONDENSER

We consider the simplest case of a condenser of the length l_1 equipped with circular fins that have the base radius R_1, the outer radius R_2, the height $R_2 - R_1$, and the constant thickness $h << R_2 - R_1$. Heat transfer across the outer fin end is neglected. The height is assumed to be proportional to the thickness: $R_2 - R_1 = A{\cdot}h$, with the factor A of the order of 5–10. Higher fins made of thermally conductive materials are unpractical because of slower heat exchange, as well as for some economic and engineering reasons [*Roizen and Dulkin, 1977*]. The number of fins (n) is

$$n = \frac{l_1}{h+s}, \qquad (1)$$

where s is the fin-to-fin spacing. The total amount of heat dissipated from the condenser to air per unit time Q_c (W) depends on the effective heat loss α_c, the total outer surface area of the condenser S_c, and the temperature difference $\Delta t_{ca} = t_c - t_a$ between the case wall (with the generatrix of the radius R_1) and the incoming air flow (where t_c and t_a are the temperatures of the condenser and air, respectively):

$$Q_c = \alpha_c S_c \Delta t_{ca}. \qquad (2)$$

The temperature t_c is constant all along the generatrix of the condenser.

The value Q_c equals the total heat extracted from all fins Q_F and all no-fin intervals Q_N. The total surface area of the condenser is found in the same way via the surface area of a single fin S_{1F} and the no-fin interval S_{1N} and their sum S_1:

$$Q_c = Q_F + Q_N;\ \ S_c = S_F + S_N = n(S_{1F} + S_{1N}) \equiv nS_1, \qquad (3)$$

while Q_R and Q_N, S_{1R} and S_{1N} are given by

$$Q_N = \alpha_a S_N \Delta t_{ca};\ \ S_N = nS_{1N} = n2\pi R_1 s, \qquad (4)$$

where the heat loss α_a for the unfinned interval is found as in the case of cross flow around tubes [*Wong, 1977*]:

$$\alpha_a = 0.0208 \frac{\lambda_a}{2R_1}\left(\frac{2R_1 V_a}{\nu_a}\right)^{0.814}. \qquad (5)$$

where λ_a, ν_a, and V_a are, respectively, the thermal conductivity and diffusivity coefficients and the velocity of incoming air flow.

$$Q_F = nQ_{1F};\ \ S_F = nS_{1F} = n2\pi\left(R_2^2 - R_1^2\right). \qquad (6)$$

Heat extracted from a single fin Q_{1F} is given by [*Wong, 1977*]:

$$Q_{1F} = 2\pi R_1 \lambda h \Delta t_{ca} \mu\psi \equiv K_{1F} \Delta t_{ca};\ \ \mu = \sqrt{\frac{2\alpha_{1a}}{\lambda h}}; \qquad (7)$$

$$\psi = \frac{I_1(\mu R_2)K_1(\mu R_1) - I_1(\mu R_1)K_1(\mu R_2)}{I_1(\mu R_2)K_0(\mu R_1) + I_0(\mu R_1)K_1(\mu R_2)}, \qquad (8)$$

where λ is the thermal conductivity of the fin material; I_0, K_0, I_1, and K_1 are the Bessel functions, while the heat loss from the fin α_{1a} is found as in the case of air flow around a plate [*Mikheev and Mikheeva, 1973*]

$$\alpha_{1a} = 0.032 \frac{\lambda_a}{2R_2}\left(\frac{2R_2 V_a}{\nu_a}\right)^{0.8}. \qquad (9)$$

With equations (1)–(4), (6), and (7), the coefficient α_c becomes

$$\alpha_c = \frac{K_{1F} + \alpha_a S_{1N}}{S_1}. \qquad (10)$$

Thus, the total heat dissipated into air from the condenser can be found with equation (2) using equation (10). However, equation (2) includes an intermediate parameter of the case wall temperature (t_c). To be related to the processes inside the cooling system, heat dissipation has to be expressed via the temperature of the saturation vapor t_s. Vapor pressure can be assumed constant to a high accuracy, all along the condenser case, given that the hydraulic resistance to vapor flow toward the condenser is very small for short tubes. Therefore, the saturation temperature t_s (related to pressure by the saturation curve) is likewise constant all along the system (condenser + evap-

orator). The vapor condensed on the condenser inner wall can be considered as an additional layer in a multi-layer wall (with the inside and outside temperatures t_s and t_a, respectively), and the total heat extracted from the fins Q_c can be expressed via the total heat loss α_{tot} and the temperature difference $\Delta t_{sa} = t_s - t_a$ as

$$Q_c = \alpha_{tot} S_c \Delta t_{sa}. \qquad (11)$$

Note that direct observations in transparent physical models show the film thickness δ to be very small ($\delta << R_1$), which allows us to use the equation for flat walls in further consideration.

In (11), α_{tot} is given by ($S_{ic} = 2\pi R_1 l_1$ is the inner surface area of the condenser case):

$$\alpha_{tot} = \left(\frac{1}{\bar{\alpha}_f} \frac{S_c}{S_{ic}} + \frac{1}{\alpha_c} \right)^{-1}, \qquad (12)$$

while the average heat loss across the condensed vapor film $\bar{\alpha}_f$ is estimated via its average thickness $\bar{\delta}$ (where λ_{cl} is the thermal conductivity of the coolant liquid phase):

$$\bar{\alpha}_f = \frac{\lambda_{cl}}{\bar{\delta}}. \qquad (13)$$

Hereafter the contribution of the condenser wall to the total thermal resistance is neglected because it is commonly made of material with high thermal conductivity and relatively thin walls.

The coefficient $\bar{\alpha}_f$ is estimated with regard to depth dependence of the film thickness $\delta(z)$, which is found using Nusselt's theory of film condensation [*Mikheev and Mikheeva, 1973*], at the constant temperature t_c. Let the origin of coordinates be on the upper surface of the condenser and the axis Oz be directed downward (Fig. 1). The depth dependence of the film thickness with regard to correction for heat exchange with air (neglecting the vapor density compared to the liquid density) is

$$\int_0^z q(z)dz = \frac{\kappa_{cl} g \rho_{cl}}{3\nu_{cl}} \delta^3(z), \qquad (14)$$

where the heat flow $q(z)$ on the condenser refers to its inner smooth surface (with the surface S_{ic}) and is:

$$q(z) = \Delta t_{sa} \Big/ \left(\frac{\delta(z)}{\lambda_{cl}} + \frac{S_{ic}}{\alpha_c S_c} \right). \qquad (15)$$

In these equations, ν_{cl}, ρ_{cl}, and κ_{cl} are, respectively, the kinematic viscosity, the liquid phase density, and the vapor-liquid transition heat of the coolant; g is the acceleration due to gravity.

Differentiation along z of both sides in (14) leads to the differential equation for $\delta(z)$ (with the initial condition $\delta(0) = 0$)

$$\frac{\nu_{cl}\Delta t_{sa}}{\kappa_{cl} g \rho_{cl}} = \left(\frac{\delta(z)}{\lambda_{cl}} + \frac{S_{ic}}{\alpha_c S_c} \right) \delta^2(z) \frac{d\delta}{dz}. \qquad (16)$$

Integration of this equation, in turn, leads to the biquadratic equation with respect to $\delta(z)$

$$\delta^4 + \frac{4\delta^3}{3} \frac{\lambda_{cl} S_{ic}}{\alpha_c S_c} - \frac{4\lambda_{cl}\nu_{cl}\Delta t_{sa} z}{\kappa_{cl} g \rho_{cl}} = 0. \qquad (17)$$

Its solution can be written in elementary functions, but it is quite cumbersome and inconvenient for further analysis. A simpler way is to take into account the small film thickness and assume that the first term in (17) is much less than the second one, i.e.,

$$\delta << \frac{4}{3} \frac{\lambda_{cl} S_{ic}}{\alpha_c S_c}. \qquad (18)$$

Note that the role of the film thermal resistance becomes insignificant if (18) fulfills, as follows from comparison of expressions (18) and (15) (the factor 4/3 being insignificant). However, (18) cannot fulfill for a condenser of high thermal performance, with the large surface S_c and high heat loss α_c, with a large dot product in the denominator of the right-hand side of (18). It means that the performance of a condenser is limited by the thermal resistance of the condensate film, even when it becomes commensurate with the resistance of the condenser. Therefore, the fulfillment of (18) places constraints on the design of finned condensers in thermosyphons and, in this respect is an economically and technologically important criterion. This requirement imposed on the condenser design has to be taken into account in further consideration.

With regard to the formulated hypothesis, we obtain the equation for the film thickness from (17), neglecting the first term in the left-hand side:

$$\delta(z) = \left(\frac{3\nu_{cl}\Delta t_{sa} z}{\kappa_{cl} g \rho_{cl}} \cdot \frac{\alpha_c S_c}{S_{ic}} \right)^{1/3}. \qquad (19)$$

The film is the thickest on the condenser bottom, at $z = l_1$. If (18) fulfills at the maximum film thickness, it obviously fulfills for any thinner film. From (18) and (19) it follows that

$$\frac{\alpha_c S_c}{S_{ic}} \left(\frac{3^4 \nu_{cl}\Delta t_{sa} l_1}{4^3 \lambda_{cl}^3 \kappa_{cl} g \rho_{cl}} \right)^{1/4} << 1. \qquad (20)$$

The left-hand side of (20) is dimensionless and depends on the coolant type, as well as on the condenser design (it is the function of the parameters h and s according to (1)–(10)). The inner and outer surface areas of an unfinned condenser are equal (the wall thickness being neglected), and the first factor in the left-hand side is equal to α_a defined by (5). Let the left-hand side of (20) be denoted as Φ with the subscript of the respective coolant. For R_1 = 16 mm, l_1 = 1.5 m and the wind speed 3 and 8 m/s, the values of α_a are 26.4 and 58.3 W/(m^2·deg), while Φ values (in these two cases) are: $\Phi_{am} = 8.26 \cdot 10^{-3}$; $1.83 \cdot 10^{-2}$

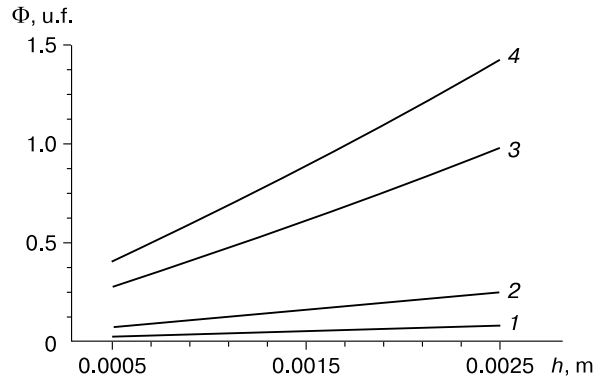

Fig. 2. Behavior of parameter Φ as a function of fin thickness (*h*) for ammonia (*1*), CO_2 (*2*), HCFC (Freon)-22 (*3*); HCFC (Freon)-12 (*4*) coolants, at R_1 = 16 mm, l_1 = 1.5 m, *s* = 0.01 m, *A* = 10.

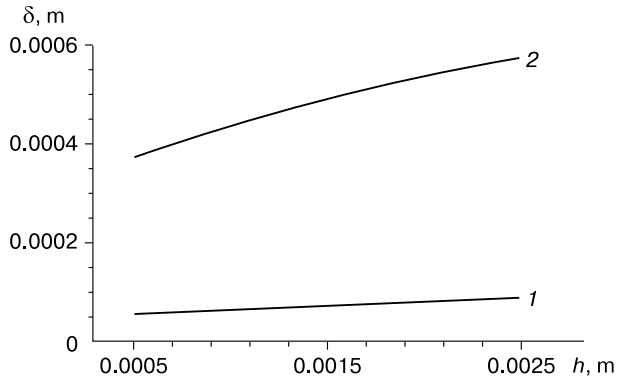

Fig. 3. Film thickness (δ) inside a condenser as a function of fin thickness (*h*) for ammonia (*1*) and HCFC (Freon)-12 (*2*) coolants.

for ammonia; $\Phi_{fr\ 12} = 1.50 \cdot 10^{-1}$; $3.33 \cdot 10^{-1}$ for Freon-12; $\Phi_{fr\ 22} = 1.04 \cdot 10^{-1}$; $2.31 \cdot 10^{-1}$ for Freon-22; and $\Phi_{CO_2} = 2.63 \cdot 10^{-2}$; $5.79 \cdot 10^{-2}$ for CO_2 (at the temperature difference about the maximum Δt_{sa} = 20 °C). Thus, (20) fulfills in all cases in the absence of fins (though not perfectly for Freons at high wind speed), and the contribution of film thickness can be neglected for all three types of coolants. On this basis, an unfinned thermosyphon was inferred to be insensitive to the coolant type [*Gorelik, 1980*]. Of course, this does not mean that an unfinned condenser is more efficient than a finned one. For instance, inequality (20) will fulfill still better for a thermally insulated unfinned condenser, but its performance will be obviously worse. On the other hand, fins on the outer surface of the condenser improve external heat exchange, but their enhancement looses sense when the thermal resistance of the film becomes significant. Note also that the film resistance is specific to convective processes with phase change, unlike the design factors which also affect the heat exchange efficiency.

For a finned condenser, the parameter Φ depends on thickness, spacing, and other parameters of fins (see the fin thickness dependence of Φ in Fig. 2 for different coolants, assuming the spacing *s* = 10 mm, *A* = 10, and the wind speed 5 m/s). For the chosen condenser design, inequality (20) fulfills well for all fin thicknesses with ammonia (Fig. 2) and slightly worse with carbon dioxide. With Freons, only very thin fins can be efficient, but they may be problematic to fabricate. Thus, the thermal resistance of a condensate film is controlled by its thickness and by the thermal conductivity of the liquid phase in different coolants. Variations of film thickness at the condenser output as a function of fin thickness for ammonia and Freon-12 (Fig. 3) show that ammonia films are at least five times thinner, have about 8 times higher thermal conductivity, and, hence, about 40 times lower thermal resistance.

As (18) fulfills, with regard to (15), the total heat loss from the condenser can be written as:

$$Q_c = \alpha_c S_c \Delta t_{sa}. \qquad (21)$$

It differs from (2) in the temperature difference.

EVAPORATOR

The thickness of the sinking condensate film continuously decreases from the maximum δ_0 at the input of the evaporator, which coincides with its maximum thickness at the condenser output and can be estimated by (19) at $z = l_1$. The depth-dependent film thickness variations for the evaporator unit likewise follow the Nusselt theory, applied to evaporation instead of condensation, at a constant temperature on the evaporator wall t_g equal to the current temperature of the ambient ground. The previously estimated [*Gorelik, 1980*] fluid flow rates inside the system largely exceed the rate of ground temperature redistribution. Therefore, the formation and flow of the film can be considered as a quasi-stationary process at the above conditions. In this case, the heat flow toward the evaporator $q(z)$ is

$$q(z) = \frac{\lambda_{cl} \Delta t_{gs}}{\delta(z)}. \qquad (22)$$

The equation of the evaporator heat budget (similar to (14)) makes basis for the differential equation of the film thickness. With the initial condition $\delta = \delta_0$ at $z = l_1 + l_0$, the equation for $\delta(z)$ becomes

$$\delta^4(z) = \delta_0^4 + \frac{4\lambda_{cl} \Delta t_{gs} \nu_{cl} \left(l_1 + l_0 - z\right)}{\kappa_{cl} \rho_{cl} g};\ l \geq z \geq l_1 + l_0, \qquad (23)$$

where l_0 is the height of the lateral heat insulation at the level of the active layer (within it the film thickness does not change), and l is the total length of the device. According to (23), the nonzero film thickness is limited by some natural depth which reasonably corresponds to the maximum length of the evaporator (see below).

Equation (23), with averaging along z, can be used to calculate the heat loss average over the evaporator $\bar{\alpha}_{if}$. Note that the parameters t_s and t_g remain unconstrained in all above equations. The saturation temperature t_s is estimated using the total heat budget for the system as a whole: heat coming to the evaporator equals that dissipating to the air from the condenser: $Q_c = Q_{ev}$, where Q_c is defined by (21), while the heat from the evaporator is $Q_{ev} = \bar{\alpha}_{if} S_{ev} \Delta t_{gs}$ (where the evaporator surface area S_{ev} is $2\pi R_1 l_2$ and its length is l_2). Solving the heat budget equation with respect to t_s gives

$$t_s = \frac{S_{ev}\bar{\alpha}_{if} t_g + S_c \alpha_c t_a}{S_{ev}\bar{\alpha}_{if} + S_c \alpha_c}. \qquad (24)$$

With (22) and (23), the average heat loss from the evaporator $\bar{\alpha}_{if}$ likewise depends on the temperature t_s and is given by

$$\bar{\alpha}_{if} = \left(\frac{\lambda_{cl}^3 \kappa_{cl} \rho_{cl} g}{4 \nu_{cl} l_2 \Delta t_{gs}} \right)^{0.25}. \qquad (25)$$

To write the equation for t_s, we first define the difference $\Delta t_{gs} = t_g - t_s$, using (24), then pick the terms with the difference Δt_{gs}, and obtain the transcendent algebraic equation with respect to Δt_{gs}:

$$\Delta t_{gs} + \frac{3}{4} \frac{S_{ev}}{\alpha_c S_c} \left(\frac{\lambda_{cl}^3 \kappa_{cl} \rho_{cl} g}{4 \nu_{cl} l_2} \right)^{0.75} \Delta t_{gs}^{0.75} = \Delta t_{ga}. \qquad (26)$$

Equation (26) is solved numerically. In the range of ground temperatures t_g from 0 °C to t_a, the temperature t_s is close to t_g to thousandths fractions for ammonia and 0.6 °C for Freon-12.

The difference Δt_{gs} cannot be neglected when estimating the maximum length of the evaporator tube. At $\delta = 0$, the maximum evaporator length l_2 is obtained from (23) as

$$l_2 = \delta_0^4 \frac{\kappa_{cl} \rho_{cl} g}{4 \lambda_{cl} \Delta t_{gs} \nu_{cl}}. \qquad (27)$$

Substituting δ_0 from (19) into (27) at $z = l_1$ and assuming the heat loss from the condenser $\alpha_c S_c / S_{ic} \equiv F$ (which enters the equation for δ_0; see its behavior as a function of fin thickness in Fig. 4) to be 40, 200 and 400 W/(m^2·deg), we obtain l_2 = 1.7; 6.0 and 11.9 m, respectively, for ammonia. For Freon-12, it can reach 200 m, which may be a major advantage of Freon evaporators in using thermosyphons for cooling deep ground.

In principle, evaporator tubes in the cooling devices for deep ground can be longer than the estimated maximum value, but their lower end should be filled with the liquid coolant. However, we have no reliable evidence of thermosyphon operation in these conditions at our disposal.

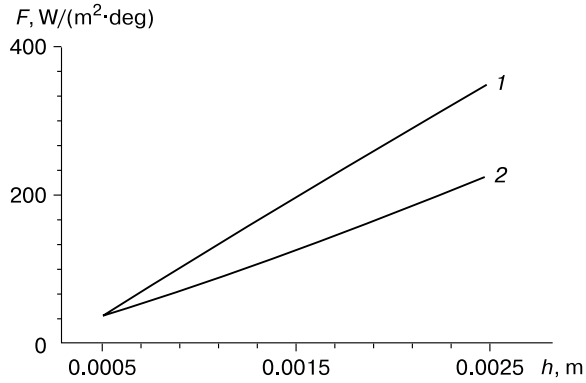

Fig. 4. Heat transfer in the condenser (parameter F) as a function of fin thickness (h) at fin spacing s = 0.005 m (*1*) and 0.01 m (*2*), at R_1 = 16 mm, l_1 = 1.5 m, A = 10.

The reported estimates for the maximum evaporator length appear to be the first calculations of this kind and require further experimental checks. This is especially important also because one of us repeatedly observed sporadic ebullition of the coolant on the evaporator bottom during laboratory testing of vertical thermosyphons in physical models with transparent walls. The vapor-liquid flow from such ebullition wets the evaporator walls and reaches the condenser, while the evaporator temperature falls abruptly, and moisture condenses on its outer wall surfaces. The process, which may play a significant role, was demonstrated in a video at TICOP [*Gorelik, 2012*], but it is not taken into account in this consideration. Testing of thermosyphons under laboratory control has to be continued. The sinking film moves wave-like as a result of interaction with the ascending counter-flow of vapor [*Kapitsa, 1948*], but the wave-like flow is stable and even improves the heat exchange to some extent [*Mikheev and Mikheeva, 1973*].

EXTERNAL PROBLEM FOR THERMAL STABILIZATION

The ground temperature field in the zone of thermal stabilization is estimated as follows. The key issue is to constrain the boundary conditions on the outer wall of the evaporator which contacts the ground. For this the saturation temperature (t_s) is expressed from the equation of total heat budget. The heat loss from the condenser Q_c is defined by the same equation (21) while the heat coming to the evaporator Q_{ev} from the ground is

$$\alpha_c S_c \Delta t_{sa} = S_{ev} \lambda_f \left(\frac{\partial t}{\partial r} \right)_{R_1}, \qquad (28)$$

where λ_f is the thermal conductivity of frozen ground; t is the ground temperature depending on the radial

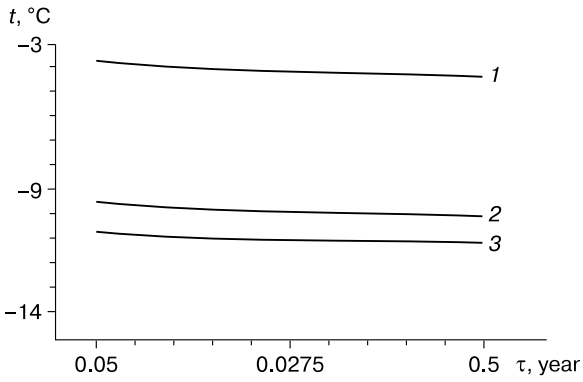

Fig. 5. Temperature on the evaporator wall (t) as a function of time (τ) for F_{tot} = 10 (*1*), 66 (*2*), and 116 (*3*) W/(m²·deg).

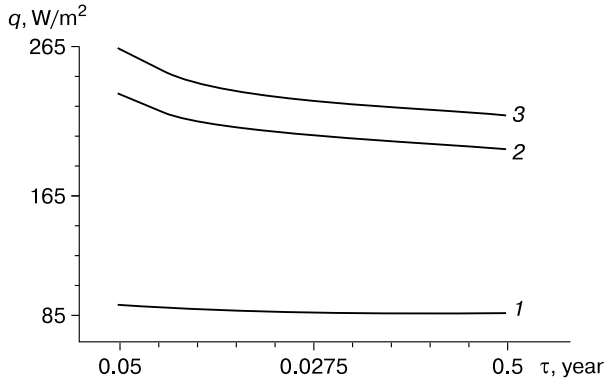

Fig. 6. Heat flow (q) as a function of time (τ) for F_{tot} = 10 (*1*), 66 (*2*), and 116 (*3*) W/(m²·deg).

coordinate r (in the axi-symmetric case) and the time τ. Taking into account the approximate equality $t_s \approx t_g$, the sought equation is

$$\frac{\alpha_c S_c}{S_{ev}}\left(t_a - t_g\right) = -\lambda_f \left(\frac{\partial t}{\partial r}\right)_{R_1}. \qquad (29)$$

The same equation was obtained earlier for an unfinned condenser [*Gorelik, 1980*], with the only difference in the factor at the temperature difference in the left-hand side of (29), which is the heat loss parameter for the device as a whole $F_{tot} = \alpha_c S_c / S_{ev}$. Therefore, the condition can be extrapolated to the case of a finned thermosyphon (in the absence of fins, $F_{tot} = \alpha_a l_1 / l_2$). This condition allows formulating and solving a large scope of problems concerning the temperature field under structures built with the use of vertical thermosyphons. Specifically, the radius of thermal effect [*Barenblatt, 1954*] can be used to estimate, to some approximation, the ground temperature dynamics or cooling efficiency as a function of thermosyphon design. The exact solution can be approximated by a series with any number of terms (the longer the series the more exact the approximation) which account for the problem symmetry and satisfy certain conditions at the domain boundaries [*Barenblatt, 1954*]. The approximate solution includes a time-dependent thermal effect radius $L(\tau)$ derived from the total heat budget equation and should satisfy the latter within this radius, instead of the thermal conductivity equation.

The problem is solved for a horizontally infinite layer of frozen soil with the initial temperature t_0 and the thickness equal to the evaporator length in a single thermosyphon inserted into this layer orthogonally to its perfectly insulated top and base surfaces. The thermal perturbation from the thermosyphon is obviously axi-symmetical and one-dimensional in this case. As it was previously shown [*Gorelik, 1980*], the approximate solution for temperature dynamics in the soil layer is

$$t(r,\tau) = \frac{\frac{\alpha_c S_c}{S_{ev}}\left(t_a - t_0\right)}{\frac{\lambda_f}{R_1} + \frac{\alpha_c S_c}{S_{ev}} \cdot \ln\frac{L(\tau)}{eR_1}} \left(\ln\frac{L(\tau)}{er} + \frac{r}{L(\tau)}\right) + t_0;$$

$$r \le L(\tau), \qquad (30)$$

where e is the natural logarithm base. Note that the temperature remains the same, equal to t_0 outside the thermal effect radius. This equation satisfies the boundary conditions at the radius $r = L(\tau)$:

$$t(L,\tau) = t_0; \ \left.\frac{\partial t}{\partial r}\right|_{L(\tau)} = 0, \qquad (31)$$

as well as to the condition (29) on the evaporator outer wall. The total heat budget condition defines the cooling expansion law:

$$L(\tau) = R_1 + \sqrt{12\mu_f \tau}, \qquad (32)$$

where μ_f is the thermal diffusivity of frozen soil. Equations (30) and (32) can be used to estimate the temperature dynamics on the evaporator wall during the period of active thermal stabilization (about six months) and heat flow toward the evaporator wall as a function of heat loss from the ground to the air, which characterize heat exchange with the ground. The two parameters are plotted as a function of time in Figs. 5 and 6, respectively, for F_{tot} = 10 (unfinned condenser), 66 and 116 W/(m²·deg).

Both the temperature (t) on the evaporator wall (Fig. 5) and the heat flow (q) toward it (Fig. 6) change little with time. Furthermore, as heat loss becomes more then 10 times higher (116 against 10 W/(m²·deg)), t and q change only by factors of 2 and 2.5, respectively, because the ground has low thermal conductivity, about that in insulators. The latter inference is illustrated in Figs. 7 and 8 by the behavior of some hypothetical soil with a higher thermal conductivity of λ_f = 30 W/(m·deg), with the

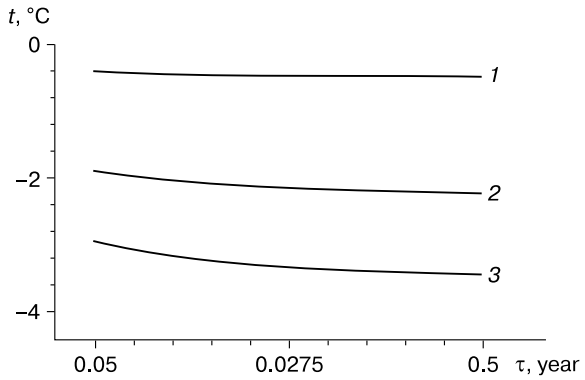

Fig. 7. Temperature on the evaporator wall (t) as a function of time (τ) for an ideal soil for F_{tot} = 10 (*1*), 66 (*2*), and 116 (*3*) W/(m²·deg).

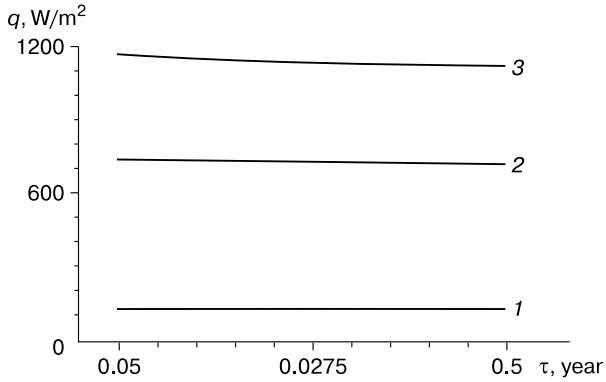

Fig. 8. Heat flow (q) as a function of time (t) for an ideal soil for F_{tot} = 10 (*1*), 66 (*2*), and 116 (*3*) W/(m²·deg).

thermospyphon parameters the same as in the case of Figs. 5 and 6. In this ideal soil, the changes are commensurate. If the ideal soil has a zero thermal conductivity, the temperature at the evaporator wall reaches its minimum, equal to air temperature, while the heat flow zeroes at all heat loss values. Inasmuch as the magnitude and thermal radius of ground cooling are the basic parameters of thermal stabilization in permafrost foundations, the performance of finned condensers should be checked as to the capacity of soil to receive and redistribute the incoming heat.

THERMAL PERFORMANCE OF THERMOSYPHONS

Thermosyphons are used to cool the ground down to the design temperature and maintain this temperature for the whole lifespan of structures built on permafrost. Note that the thermal stabilization effect from natural heat convection during the active period (winter) almost fully disappears in the end of the passive period (summer). Solution (30) allows estimating the cooling effect for arbitrary heat loss by superposition of two heat sources: one causes an effect defined by (30), while the effect of the other, which is started in the end of the cold season, is of the same magnitude but opposite polarity [*Gorelik and Meltser, 1980*]. Thus, for the same F_{tot} of 10, 66 and 116 W/(m²·deg), we obtain residual cooling within −0.3 °C in the end of the warm season, irrespective of the assumed heat loss. This estimate is approximate because the assumed heat insulation along the top and base of the soil layer rules out upward and downward heat sinks. The solution is shown in Fig. 9, *a*, *b* for a uniform halfspace, with a single thermosyphon at F = 116 W/(m²·deg), assuming t_0 = −1 °C. The boundary condition on the ground surface can be specified as periodic (seasonal) variations either in ground temperature or in heat flow, depending on the available data and studied processes in the active layer.

Anyway, such boundary conditions should provide constant ground temperature at the depth of zero annual amplitudes (10–15 m) for the whole lifes-

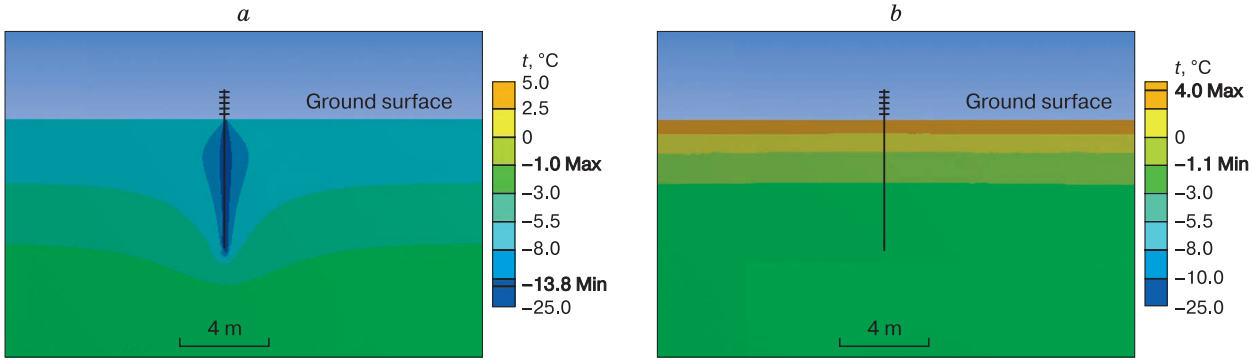

Fig. 9. Temperature field in the zone of thermal stabilization by a single thermosyphon in the end of winter (*a*) and summer (*b*) seasons, at F = 116 W/(m²·deg).

Color scale on the right corresponds to ground temperature. *Max* and *Min* refer, respectively, to maximum and minimum temperatures inside the modeling domain.

pan of the structures, about 20–30 years. The test example does not include the structure itself, otherwise an uncontrollable effect of the boundary condition on the calculation results may cause a significant error. Since we focus mainly on the action of the thermosyphon itself, it is enough to assume constant temperature equal to the initial ground temperature (–1 °C) on the upper boundary, whereby the conditions for the depth of zero annual amplitude will fulfill automatically. The annual air temperature pattern is specified independently of the ground temperature on the upper surface and assumed to be constant, at the winter mean (–15 °C) between the beginning of November to end of April; condition (29) on the evaporator wall applies to this period as well. During the warm season (from May to end of October), heat flow to the evaporator is assumed to be zero. The modeling domain is cylindrical, with its vertical axis coinciding with that of the themosyphon, the radius 30 m, and the depth 40 m. Each of these dimensions notably exceeds the cooling radius per year. Heat flow at the boundaries is zero.

Figure 9, *a* shows the temperature distribution around a single thermosyphon in the end of winter, when the mean temperature on the evaporator wall reaches –13 °C. The cooling effect almost fully disappears in the end of summer (Fig. 9, *b*), while the mean evaporator temperature returns to the initial value –1 °C (accurate to a tenth).

On the other hand, the bearing capacity of foundations is estimated proceeding from the highest ground temperature over the year [*Construction Rules, 2008*]. Therefore, the residual cooling effect being too small, the cold stored in the winter season cannot be included into design but only enters the factor of safety of the structures. However, this conclusion is valid for a single thermosyphon, whereas the situation is quite different in the case of multiple thermosyphons, appoximately as many as piles, used for cooling elongate buildings or structures. Multiple thermosyphons cool down a large volume of soil, which heats up much more slowly than that around a single thermosyphon, and residual cooling may reach several degrees [*Gorelik and Izmailov, 1984*]. The predicted effect was confirmed during testing near Vorkuta [*Alexandrov, 1985*].

It is also important that the effect of multiple thermosyphons weakly depends on the performance of a single device [*Gorelik, 2005*], which creates significant engineering and economic advantages for unfinned thermosyphons. Namely, it allows avoiding additional costs for drilling (as unfinned thermosyphons, both evaporators and condensers, can be installed inside piles [*Gorelik et al., 2015*]), for base metals spent on fins, and for special fin-thermosyphon coupling technology. With unfinned thermosyphons installed in piles, ventilated cellars have more space and the buildings look much better aesthetically. Some problem may arise because ice films may form on the outer surfaces of piles that host active thermosyphons and reduce their bearing capacity [*Mirenburg and Fedoseev, 1983*]. However, the known cases are restricted to a few laboratory tests with soils deformed by freezing. We are aware that further research in this line is required, but this study focuses on cooling and thermal stabilization of frozen ground where moisture migration producing ice films is largely suppressed.

The suggested approach to thermal stabilization has been supported by successful experience with evaporators installed inside buried piles (but with condensers placed outside): hundreds of thousand piles that support the Trans-Alaska pipeline system [*Khrustalev et al., 1983*], thousands of piles carrying constructions in Mirnyi city [*Makarov, 1985*] and other structures in Arctic areas [*Minkin, 2005; Dolgikh, 2014*].

CONCLUSIONS

Joint analysis of heat and mass transfer inside and outside vertical two-phase cooling systems based on natural convection (thermosyphons or Long's tubes) allows the following inferences.

1. The use of fins to enhance thermal performance is limited by the thermal resistance of condensate films sinking along the condenser inner walls. This resistance largely depends on the coolant type (being the lowest with ammonia and the highest with Freon-12) but is vanishing at any currently used coolant in the absence of fins.

2. The maximum length of the evaporator tube, estimated for the first time, corresponds to zero thickness of the condensate film (evaporator drying) and depends on the coolant and fin parameters.

3. Finning does not change much the performance of thermosyphons, estimated from the temperature and heat flow on the evaporator wall during the cold season, because soil commonly has a low thermal conductivity about that in heat insulators. Calculations for an ideal soil with its thermal conductivity about 15 times as great as the real value show the cooling effect to increase proportionally to the surface area the fins add to the condenser. Therefore, the size and spacing of fins should be designed in accordance with thermal conductivity of specific soils.

4. The applied joint analysis of heat exchange inside and outside thermosyphons allowed estimating the boundary conditions on the outer evaporator wall for finned condensers, in the same way as it was obtained previously for the unfinned case. The result makes basis for estimating the temperature field in permafrost foundations stabilized by thermosyphons.

5. The residual cooling around a single thermosyphon in the end of the warm season is within tenths of a degree and is almost insensitive to finning. The

residual cooling effect being too small, the cold stored in the winter season cannot be included into design but only enters the factor of safety of the structures. However, this conclusion is valid for a single thermosyphon, whereas the situation is quite different in the case of multiple thermosyphons, appoximately as many as piles, used for cooling long buildings or structures. The effect weakly depends on the parameters of fins.

6. Therefore, unfinned thermosyphons are no less efficient than the finned systems, but have significant engineering and economic advantages due to avoiding additional costs. This expands the applicability of thermosyphons in permafrost foundations.

We are pleased to thank Professor Lev Khrustalev for the thoughtful review of our manuscript and useful comments.

The study was supported by grant SS-3929.2014.5 for leading science schools from the President of the Russian Federation and was carried out as part of Basic Research Program 11 of the Geosciences Department of the Russian Academy of Sciences.

References

Alexandrov, Yu.A., 1985. Cooling of viscous frozen soils by a pad of vapor-liquid cooling devices, in: Geocryological Prediction in Construction Development. Proc. All-Russian Conf., Gosstroy SSSR, Vorkuta, Book 2, pp. 283–286. (in Russian)

Arnold, L.V., Mikhailovskiy, G.A., Seliverstov, V.M., 1979. Engineering Thermodynamics and Heat Transfer. Vysshaya Shkola, Moscow, 445 pp. (in Russian)

Barenblatt, G.I., 1954. Some approximate methods in the theory of 1D unsteady fluid filtration in elastic conditions. Izv. AN SSSR. Ser. Teckhn. Nauk, No. 9, 35–49.

Construction Rules, 2008. Working Document SP 25.13330.2012. Basements and Foundations in Permafrost. Minregionrazvitiya, Moscow, 140 pp. (in Russian)

Dolgikh, G.M. (Ed.), 2014. Systems for Thermal Stabilization of Permafrost. A Collection of Papers by Specialists from *Fundamentstroiarkos* R&D Company for 2010–2014. Geo Publishers, Novosibirsk, 218 pp. (in Russian)

Dolgikh, G.M., Dolgikh, D.G., Okunev, S.N., 2004. Freezing of soils: Engineering solutions of *Fundamentstroiarkos* Company, in: The Cryosphere of Petroleum Provinces. Proc. Intern. Conf., Tyumen', p. 56. (in Russian)

Dolgikh, G.M., Okunev, S.N., 2006. Construction and stabilization of cooled foundations in permafrost by *Fundamentstroiarkos* Company: Promising engineering solutions, in: Theory and Practice of Permafrost Assessment and Predictions. Proc. Intern. Conf., Tyumen', Book 2, pp. 228–232. (in Russian)

Gorelik, J.B., 1980. Modeling ground temperature field around vapor-liquid thermal piles. Probl. Nefti i Gaza Tyumeni, Issue 47, 58–61.

Gorelik, J.B., 2005. Pile basements for fundamental structures in high-latitude oil and gas fields. Gazovaya Promyshlennost`, No. 1, 82–84.

Gorelik, J.B., 2012. Laboratory study of the devices for termostabilization of frozen ground, in: Proc. 10th Intern. Conf. on Permafrost (TICOP), Pechatnik, Salekhard, p. 10.

Gorelik, J.B., Izmailov, I.G., 1984. Pre-construction ground cooling with thermal piles. Problemy Nefti i Gaza Tyumeni 61, 85–88.

Gorelik, J.B., Meltser, M.S., 1980. Ground temperature assessment for construction with the use of thermosyphons, in: Construction for Oil Production, VNIIOENG, Moscow, pp. 19–20. (in Russian)

Gorelik, J.B., Melnikov, V.P., Fakhretdinov, I.Z., Shtol, V.F., Gorelik, R.J., 2015. Patent RU 150908 U1. A Device for Thermal Stabilization of Ground. Otkrytiya. Izobreteniya, No. 7.

Kapitsa, P.L., 1948. Wave flow of thin liquid layers. Zhurnal Teoreticheskoy Fiziki 18 (1), 3–18.

Khrustalev, L.N., Ershov, E.D. (Eds.), 1999. Fundamentals of Geocryology. Part 5. Engineering Geocryology. Moscow University, Moscow, 518 pp. (in Russian)

Khrustalev, L.N., Yanchenko, O.M., Naumova, L.A., 1983. Use of autonomous vapor-liquid cooling devices in construction on permafrost: Experience and Prospects, in: Vyalov, S.S. (Ed.), Regulation of Ground Temperature Using Thermosyphons. IM SO RAN, Yakutsk, pp. 3–12. (in Russian)

Kutvitskaya, N.B., Minkin, M.A., 2014. Design of foundations for infrastructure of oil, gas, and condensate field in complex permafrost conditions. Osnovaniya, Fundamenty, Mekhanika Gruntov, No. 1, 21–25.

Long, E.L., 1964. Patent 3217791 US. Means for Maintaining Permafrost Foundations. Filed July 30, Ser. No. 386341 (Cl. 16545).

Makarov, V.I., 1985. Thermosyphons in High-Latitude Construction Engineering. Nauka, Novosibirsk, 169 pp. (in Russian)

Mikheev, M.A., Mikheeva, I.M., 1973. Fundamentalas of Heat Transfer. Energiya, Moscow, 320 pp. (in Russian)

Minkin, M.A., 2005. Basements and Foundations in Permafrost. GASIS, Moscow, 213 pp. (in Russian)

Mirenburg, Yu.S., Fedoseev, Yu.G., 1983. Interaction of thermal piles with frozen foundations, in: Vyalov, S.S. (Ed.), Regulation of Ground Temperature Using Thermosyphons. IM SO RAN, Yakutsk, pp. 82–88. (in Russian)

Roizen, L.I., Dulkin, I.N., 1977. Thermal Design of Finned Surfaces. Energiya, Moscow, 255 pp. (in Russian)

Vyalov, S.S. (Ed.), 1983. Regulation of Ground Temperature Using Thermosyphons. IM SO RAN, Yakutsk, 124 pp. (in Russian)

Wong, H.Y., 1977. Handbook of Essential Formulae and Data on Heat Transfer for Engineers. Longman, London; New York, 236 pp.

Received June 18, 2015